

Application of Energy Storage Systems for Frequency Regulation Service

Yanan Sun, Shahab Bahrami, Vincent W.S. Wong, and Lutz Lampe

Department of Electrical and Computer Engineering, The University of British Columbia, Vancouver, Canada

e-mail: {ynsun, bahramis, vincentw, lampe}@ece.ubc.ca

Abstract—Frequency control aims to maintain the nominal frequency of the power system through compensating the generation-load mismatch. In addition to fast response generators, energy storage systems can be exploited to provide frequency regulation service due to their fast ramping characteristic. In this paper, we propose a solution to leverage energy storage systems deployed in the distribution networks for secondary frequency regulation service by considering the uncertainty in system disturbances, the energy storage availability, and the AC power flow model. In particular, we tackle the uncertainty in the frequency deviations and alleviate the problem associated with the limited energy storage capacity by using a risk minimization technique. We formulate a linear program to determine the frequency regulation signals to schedule the energy storage systems by adopting the concept of conditional value-at-risk (CVaR). It enables us to minimize the risk of deviation from the nominal frequency after performing frequency regulation, while satisfying the operation constraints of the distribution network. Simulations are performed on an IEEE 37-bus test feeder with three energy storage systems that participate in the frequency regulation service. Results show that by using the proposed approach, the charging/discharging of the energy storage systems can be scheduled to regulate the frequency, and the risk of energy storage systems not being able to contribute to future regulation service can be reduced.

I. INTRODUCTION

With the fast proliferation of intermittent renewable energy sources and fluctuations in load demand, power systems need to withstand an increasing number of disturbances that may affect the system frequency. This requires a series of control actions over a continuum of time using different strategies [1]. When the system frequency deviates from its nominal value (e.g., 50 Hz), the primary frequency control takes place within the first few seconds to stabilize the interconnections. The secondary frequency control is then used to restore the system frequency to its nominal value. The system operator uses automatic generation control (AGC) to compute the area error control (ACE) signals for frequency regulation. The ACE signals indicate the amount of active power that should be injected into or absorbed from the power grid in order to restore the system frequency to its nominal value. The evolving regulatory frameworks such as the recent orders issued by the United States (U.S.) Federal Energy Regulatory Commission (FERC) open the ancillary services market for new technologies such as energy storage systems [2]–[4]. Specifically, the fast ramping characteristic of energy storage systems makes them an attractive alternative to provide rapid and accurate

frequency regulation in response to the ACE signals issued by the system operator.

There are several challenges for the system operator to leverage energy storage systems for secondary frequency regulation service. First, the system operator has uncertainty about the system disturbances, and thus the frequency changes in real-time operation. The intended service operation cycle should be divided into short frequency control intervals for the system operator to compensate frequency deviations in time if needed. Second, in each frequency control time slot, computing the ACE signal for regulation service is nontrivial as it depends on the power flow changes in the distribution networks, which are affected by the charging demand fluctuations in the energy storage systems to provide regulation service. Third, the power flow constraints in the distribution network can limit the scheduling flexibility of energy storage systems for frequency regulation. The system operator needs to satisfy the operation constraints imposed by the distribution network for providing secondary frequency regulation service. Fourth, an energy storage system may not be able to participate in the regulation service due to the limited battery capacity. Specifically, the scheduling decision of an energy storage system in each control time slot affects the amount of its stored energy, and thus the amount of its contributions in the frequency regulation during the upcoming time slots.

There have been some efforts to address the aforementioned challenges. Chen *et al.* analyzed the frequency regulation response by using energy storage systems with different penetration rates given various system disturbance levels [5]. Zhang *et al.* compared the performance of using energy storage systems to compensate frequency deviations in a single-area system with conventional generators [6]. Zhang *et al.* proposed a framework to analyze the optimal planning and control strategy of using energy storage systems for frequency regulation service at the minimum operation cost [7]. Yao *et al.* adopted a robust optimization framework to schedule energy storage systems for frequency regulation service to maximize the financial profits under the performance-based compensation scheme [8]. He *et al.* proposed a real-time cooperation scheme to coordinate wind turbines and energy storage systems for frequency regulation [9]. Tan *et al.* designed an adaptive feedback control scheme for energy storage systems to coordinate with wind turbines for providing reliable frequency ancillary service [10]. In general, the participation of the energy storage systems in frequency regulation is an optimal

control problem, where the regulation signals that are computed based on generation-load mismatch are used for scheduling decisions. However, optimizing across frequency regulation and limited energy storage capacity requires a proper design of the regulation signals, where the energy storage availability given the uncertainty in system frequency deviations should be addressed. Furthermore, the constraints imposed by the distribution network should also be considered.

In this paper, we aim to exploit energy storage systems in the distribution network for secondary frequency control to minimize the risk of deviation from the nominal value after performing frequency regulation. The main contributions of this paper are summarized as follows:

- We determine the ACE signals to schedule the energy storage systems to provide frequency regulation service by considering the uncertainty in the system disturbances, the availability of the energy storage systems, and the operation constraints imposed by the distribution network.
- We introduce a risk assessment technique to tackle the limited capacity of the energy storage systems. In particular, we adopt the concept of conditional value-at-risk (CVaR) to limit the risk of energy storage systems not being able to contribute to regulation service, given the uncertainty in the frequency deviations.
- We evaluate the performance of the proposed frequency regulation approach using simulations on an IEEE 37-bus test feeder with three energy storage systems to provide frequency regulation. We compare the performance when different energy storage capacities are considered. Results show that our risk-averse model based on CVaR successfully reduced the impact of limited energy storage on restoring the frequency to its nominal value for regulation service.

The rest of the paper is organized as follows. Our system model, including the distribution network model and energy storage system's constraints, is introduced in Section II. The scheduling problem of energy storage systems incorporated with CVaR is discussed in Section III. Simulation results and performance evaluations of the proposed framework are presented in Section IV. Section V concludes the paper.

II. SYSTEM MODEL

Consider a distribution network with a set of buses \mathcal{N} and a set of branches $\mathcal{L} \subseteq \mathcal{N} \times \mathcal{N}$. It consists of some generators, loads, and energy storage systems. Let $\mathcal{N}^s \subseteq \mathcal{N}$ denote the set of buses with energy storage system. The distribution network is connected to the transmission network through a substation bus. We model the transmission network by an equivalent virtual generator that can inject/absorb active and reactive power into/from the distribution network [11]. This generator models the power flow between the distribution and transmission networks. The system operator is responsible for monitoring the real-time system operation including the power grid's frequency and power flow. We divide the operation cycle into set $\mathcal{T} = \{1, \dots, T\}$ of T time slots. Each time slot corresponds to a short frequency control interval (e.g.,

15 minutes), during which the system operator performs frequency regulation.

At the beginning of time slot $t \in \mathcal{T}$, the system operator observes the system frequency deviation and activates the primary frequency control. The participating generators will respond within few seconds (e.g., 10 seconds). Although the primary frequency control can maintain the frequency within a certain range, it may not be able to restore the system frequency to its nominal value. Let $\Delta\omega(t)$ denote the system frequency deviation from the nominal value after performing the primary frequency regulation in time slot t . In the next step, the system operator uses the energy storage systems for the secondary frequency control to restore the system frequency. Let $\Delta\omega^{\text{reg}}(t)$ denote the change in the system frequency in time slot t after performing the secondary frequency regulation. If $\Delta\omega^{\text{reg}}(t) = -\Delta\omega(t)$, the system frequency is restored to its nominal value. The system operator computes the ACE signal for each bus with energy storage system to obtain the amount of active power that the corresponding energy storage system should absorb from or inject into the power grid. In the following subsection, we discuss how the system operator can determine the ACE signals.

A. Computing the ACE Signal

To achieve the frequency change $\Delta\omega^{\text{reg}}(t)$ in time slot $t \in \mathcal{T}$, the system operator determines the ACE signal for each bus. If the energy storage systems participate in the frequency regulation service, the power flow in the distribution lines will change. In particular, the injected active power at bus $n \in \mathcal{N}$ in time slot $t \in \mathcal{T}$ will change from its scheduled value $\bar{p}_n^{\text{inj}}(t)$ to $p_n^{\text{inj}}(t)$ after performing the frequency regulation. Let $\Delta p_n^{\text{inj}}(t) = p_n^{\text{inj}}(t) - \bar{p}_n^{\text{inj}}(t)$ denote the change in the injected active power at bus $n \in \mathcal{N}$ in time slot $t \in \mathcal{T}$ after performing the secondary frequency regulation.

In time slot $t \in \mathcal{T}$, the ACE signal corresponding to the energy storage system at bus $n \in \mathcal{N}^s$ is equal to the change in the charging demand from the scheduled value $\bar{p}_n^s(t)$ to $p_n^s(t)$. We have [12, p. 489]

$$\beta_n \Delta\omega^{\text{reg}}(t) + \Delta p_n^{\text{inj}}(t) = \bar{p}_n^s(t) - p_n^s(t), \quad n \in \mathcal{N}^s, \quad (1)$$

where β_n is the frequency bias factor of bus $n \in \mathcal{N}$. It depends on the characteristics of the generator and load connected to bus n . In particular, for the secondary frequency control, the generator at bus $n \in \mathcal{N}$ can be modeled by its speed-droop characteristic ϕ_n , which reflects the speed regulation due to governor actions [12, p. 477]. The load at bus $n \in \mathcal{N}$ can be modeled by its damping coefficient ψ_n , which is the ratio between the change in the load and the change in the frequency [12, p. 473]. The frequency bias factor of bus n can be obtained as $\beta_n = \frac{1}{\phi_n} + \psi_n$.

Equation (1) implies that when the ACE signal for a bus with energy storage system is positive (negative), the energy storage system decreases (increases) its charging power and provides regulation up (down) service.

The ACE signal is zero if there is no energy storage system

at bus n in time slot $t \in \mathcal{T}$. We have

$$\beta_n \Delta\omega^{\text{reg}}(t) + \Delta p_n^{\text{inj}}(t) = 0, \quad n \in \mathcal{N} \setminus \mathcal{N}^s. \quad (2)$$

Computing the ACE signals and the frequency change $\Delta\omega^{\text{reg}}(t)$ in (1) and (2) is a nontrivial task as it depends on the distribution network power flow. In the following subsection, we provide a linearized AC power flow model to determine the change in the injected active power into the buses during the frequency regulation service.

B. Distribution Network Model

In a distribution network, the ratio between the resistance and inductance of the lines can be large. Hence, the system operator uses AC power flow model in the distribution network. The AC power flow equations are non-convex and difficult to be solved in a timely fashion. Similar to [13], we use a linear model to approximate the AC power flow in the distribution network. Let $\mathbf{p}^{\text{inj}}(t) = (p_n^{\text{inj}}(t), n \in \mathcal{N})$ and $\mathbf{q}^{\text{inj}}(t) = (q_n^{\text{inj}}(t), n \in \mathcal{N})$ denote the vectors of injected active power $p_n^{\text{inj}}(t)$ and reactive power $q_n^{\text{inj}}(t)$ into bus $n \in \mathcal{N}$ in time slot $t \in \mathcal{T}$, respectively. Let $\mathbf{v}(t) = (|v_n(t)|, n \in \mathcal{N})$ and $\boldsymbol{\theta}(t) = (\theta_n(t), n \in \mathcal{N})$ denote the vectors of voltage magnitude $|v_n(t)|$ and phase angle $\theta_n(t)$ of bus $n \in \mathcal{N}$ in time slot $t \in \mathcal{T}$, respectively. Given the real and reactive parts of the entry (nm) in bus admittance matrix Y , denoted by G_{nm} and B_{nm} , respectively, as well as the shunt susceptance and conductance at bus n , denoted by b_{nn} and g_{nn} , respectively, the linearized AC power flow model in time slot $t \in \mathcal{T}$ is obtained as follows

$$\begin{bmatrix} \mathbf{p}^{\text{inj}}(t) \\ \mathbf{q}^{\text{inj}}(t) \end{bmatrix} = \begin{bmatrix} -\mathbf{B}' & \mathbf{G}' \\ -\mathbf{G} & -\mathbf{B} \end{bmatrix} \begin{bmatrix} \boldsymbol{\theta}(t) \\ \mathbf{v}(t) \end{bmatrix}, \quad (3)$$

where the n th diagonal element of matrices \mathbf{B} and \mathbf{B}' is B_{nn} and $B_{nn} - b_{nn}$, respectively. The non-diagonal element in row n and column m of \mathbf{B} and \mathbf{B}' is B_{nm} . Similarly, the n th diagonal element of matrices \mathbf{G} and \mathbf{G}' is G_{nn} and $G_{nn} - g_{nn}$, respectively, and the non-diagonal element in row n and column m of \mathbf{G} and \mathbf{G}' is G_{nm} .

In time slot $t \in \mathcal{T}$, the linearized active and reactive power flow through line $(n, m) \in \mathcal{L}$ with resistance R_{nm} and reactance X_{nm} can be obtained as follows.

$$p_{nm}(t) = \frac{R_{nm} (|v_n(t)| - |v_m(t)|) + X_{nm} (\theta_n(t) - \theta_m(t))}{R_{nm}^2 + X_{nm}^2}, \quad (4)$$

$$q_{nm}(t) = \frac{X_{nm} (|v_n(t)| - |v_m(t)|) - R_{nm} (\theta_n(t) - \theta_m(t))}{R_{nm}^2 + X_{nm}^2}. \quad (5)$$

The apparent power flow $s_{nm}(t) = \sqrt{p_{nm}^2(t) + q_{nm}^2(t)}$ is upper bounded by s_{nm}^{max} . This constraint can be linearized by a piecewise approximation of the circular boundary using a regular polygon with central angle α . For $(n, m) \in \mathcal{L}$, we have

$$p_{nm}(t) \cos(h\alpha) + q_{nm}(t) \sin(h\alpha) \leq s_{nm}^{\text{max}}, \quad (6)$$

where $h = \{0, 1, \dots, \frac{2\pi}{\alpha}\}$. The voltage magnitude at bus $n \in \mathcal{N}$ in time slot $t \in \mathcal{T}$ is bounded by the limits v_n^{min} and v_n^{max} .

We have

$$v_n^{\text{min}} \leq |v_n(t)| \leq v_n^{\text{max}}. \quad (7)$$

Constraints (3)–(7) can be used by the system operator to determine the feasible power flow within the distribution network during the secondary frequency regulation in time slot t . There are some operation constraints for an energy storage system, which are described in the following subsection.

C. Energy Storage System's Operation Constraints

In time slot $t \in \mathcal{T}$, the power rating of the energy storage system at bus $n \in \mathcal{N}^s$ has limits $p_n^{\text{s,min}} < 0$ and $p_n^{\text{s,max}} > 0$.

$$p_n^{\text{s,min}} \leq p_n^{\text{s}}(t) \leq p_n^{\text{s,max}}, \quad n \in \mathcal{N}^s. \quad (8)$$

Besides, the change in the charging power of an energy storage system is subject to the ramp up and down rating limits $\Delta p_n^{\text{s,min}} < 0$ and $\Delta p_n^{\text{s,max}} > 0$ due to the limits in its mechanical inertia. For $t \in \mathcal{T} \setminus \{1\}$, we have

$$\Delta p_n^{\text{s,min}} \leq p_n^{\text{s}}(t) - p_n^{\text{s}}(t-1) \leq \Delta p_n^{\text{s,max}}, \quad n \in \mathcal{N}^s, \quad (9)$$

and $\Delta p_n^{\text{s,min}} \leq p_n^{\text{s}}(1) \leq \Delta p_n^{\text{s,max}}$, $n \in \mathcal{N}^s$. If there is no energy storage system connected to bus $n \in \mathcal{N} \setminus \mathcal{N}^s$, then $p_n^{\text{s,min}} = p_n^{\text{s,max}} = 0$. Let $E_n^{\text{init}} \geq 0$ denote the initial energy level of the energy storage system at bus $n \in \mathcal{N}^s$ at the beginning of the operating cycle \mathcal{T} . The stored energy in the battery until time slot $t \in \mathcal{T}$ is nonnegative and upper bounded by the limit E_n^{max} . We have

$$0 \leq E_n^{\text{init}} - \sum_{k=1}^t p_n^{\text{s}}(k) \leq E_n^{\text{max}}, \quad n \in \mathcal{N}^s. \quad (10)$$

Constraints (8)–(10) guarantee that the energy storage systems operate within their physical range to provide regulation.

III. PROBLEM FORMULATION AND SOLUTION APPROACH

In this section, we present how the system operator determines the charging/discharging of the energy storage systems to provide secondary frequency regulation service. Constraints (9) and (10) imply that the operation of an energy storage system in *current* time slot $t \in \mathcal{T}$ affects its energy level during the *upcoming* time slots $\mathcal{T}(t+1) = \{t+1, \dots, T\} \subset \mathcal{T}$. Hence for the frequency regulation in current time slot t , the system operator needs to take into account the changes in the charging/discharging power of the energy storage systems over current time slot t and upcoming time slots $k \in \mathcal{T}(t+1)$. If the system operator is aware of the profile of the system frequency deviations $\Delta\boldsymbol{\omega}(t) = (\Delta\omega(t), \dots, \Delta\omega(T))$, then it can solve the following optimization problem to determine the charging/discharging profile $\mathbf{p}_n^{\text{s}}(t) = (p_n^{\text{s}}(t), \dots, p_n^{\text{s}}(T))$ of the energy storage system at bus $n \in \mathcal{N}^s$.

$$\begin{aligned} & \underset{\substack{\mathbf{p}_n^{\text{s}}(t), n \in \mathcal{N}^s, \\ \Delta\omega^{\text{reg}}(\tau), \tau \in \{t, \dots, T\}}}{\text{minimize}} & \sum_{\tau=t}^T |\Delta\omega^{\text{reg}}(\tau) + \Delta\omega(\tau)| \end{aligned} \quad (11)$$

subject to constraints (1)–(10) for time slots $\{t, \dots, T\}$,

where $|\cdot|$ is the absolute value. Note that the system operator may not be able to restore the system frequency to its nominal value (i.e., $\Delta\omega^{\text{reg}}(\tau) \neq -\Delta\omega(\tau)$ for the time slots $\tau \in$

$\{t, \dots, T\}$) due to the constraints imposed by the distribution network and the energy storage systems. Therefore, in problem (11), the system operator aims to minimize the difference between the regulated frequency and the system frequency deviations. In problem (11), it is assumed that the system operator is aware of the profile of the system frequency deviations $\Delta\omega(t)$. However, in practice, the system operator observes only the actual system frequency deviation in current time slot t and has uncertainty about the frequency changes in upcoming time slots $k \in \mathcal{T}(t+1)$. The system operator can use the historical data record of the system frequency fluctuations to obtain a *presumed* frequency deviation profile $\Delta\hat{\omega}(t+1)$ for the underlying system. Nevertheless, the presumed system frequency deviation profile $\Delta\hat{\omega}(t+1) = (\Delta\hat{\omega}(t+1), \dots, \Delta\hat{\omega}(T))$ may be different from the realized frequency deviation profile $\Delta\omega(t+1) = (\Delta\omega(t+1), \dots, \Delta\omega(T))$ in upcoming slots $k \in \mathcal{T}(t+1)$. Hence, the system operator needs to implement a proper mechanism to determine the close-to-actual frequency deviation profile $\Delta\hat{\omega}(t+1)$ using the historical data record.

We introduce the risk measure CVaR to determine the presumed profile $\Delta\hat{\omega}(t+1)$. The system operator can use CVaR to limit the *likelihood* of large difference between the presumed frequency deviation profile $\Delta\hat{\omega}(t+1)$ and the realized frequency deviation profile $\Delta\omega(t+1)$. Note that for upcoming time slots $k \in \mathcal{T}(t+1)$, the presumed deviation value $\Delta\hat{\omega}(k)$ may be different from the actual frequency deviation of the system $\Delta\omega(k)$. Let $f(\Delta\hat{\omega}(t+1), \Delta\omega(t+1))$ denote a real-valued function that captures the difference between the profile of presumed frequency changes $\Delta\hat{\omega}(t+1)$ and the profile of realized frequency changes $\Delta\omega(t+1)$. For $t \in \mathcal{T} \setminus \{T\}$, we have

$$f(\Delta\hat{\omega}(t+1), \Delta\omega(t+1)) = \sum_{k=t+1}^T |\Delta\hat{\omega}(k) - \Delta\omega(k)|. \quad (12)$$

Given the confidence level $\delta \in (0, 1)$ and vector $\Delta\hat{\omega}(t+1)$ in time slot $t \in \mathcal{T}$, we define the value-at-risk (VaR) as

$$\text{VaR}_\delta(\Delta\hat{\omega}(t+1)) = \min\{\eta \mid \Pr\{f(\cdot) \geq \eta\} < 1 - \delta\}, \quad (13)$$

where η is the minimum threshold, for which the probability that $f(\Delta\hat{\omega}(t+1), \Delta\omega(t+1)) \geq \eta$ is less than $1 - \delta$. For the confidence level $\delta \in (0, 1)$ and vector $\Delta\hat{\omega}(t+1)$ in time slot $t \in \mathcal{T}$, the CVaR can be defined as follows

$$\text{CVaR}_\delta(\Delta\hat{\omega}(t+1)) \triangleq \mathbb{E}\{f(\Delta\hat{\omega}(t+1), \Delta\omega(t+1)) \mid f(\Delta\hat{\omega}(t+1), \Delta\omega(t+1)) \geq \text{VaR}_\delta(\Delta\hat{\omega}(t+1))\}, \quad (14)$$

where $\mathbb{E}\{\cdot\}$ is the expectation over the random variable $\Delta\omega(t+1)$. CVaR is a convex function and can be minimized using sampling techniques especially when the probability distribution of the uncertain variables is not available [14]. Note that CVaR is the expectation over the scenarios, where $f(\Delta\hat{\omega}(t+1), \Delta\omega(t+1))$ is greater than VaR. Thus, CVaR is always greater than or equal to VaR, and minimizing CVaR results in a low VaR as well.

We use the set of $\mathcal{J} \triangleq \{1, \dots, J\}$ samples $\Delta\omega^j(t+1)$ of

the random variable $\Delta\omega(t+1)$ from the historical record. We obtain $\Pr\{\Delta\omega^j(t+1)\}$, the probability of the scenario with sample $\Delta\omega^j(t+1)$. The CVaR for confidence level δ and vector $\Delta\hat{\omega}(t+1)$ can be obtained as [14]

$$\text{CVaR}_\delta(\Delta\hat{\omega}(t+1)) = \min_{\eta \in \mathbb{R}} \Gamma_\delta(\Delta\hat{\omega}(t+1), \eta), \quad (15)$$

where

$$\Gamma_\delta(\Delta\hat{\omega}(t+1), \eta) = \eta + \sum_{j \in \mathcal{J}} \frac{\Pr\{\Delta\omega^j(t+1)\}}{(1-\delta)} [f(\Delta\hat{\omega}(t+1), \Delta\omega^j(t+1)) - \eta]^+. \quad (16)$$

The system operator introduces function $\Gamma_\delta(\Delta\hat{\omega}(t+1), \eta)$ with a weight coefficient $\kappa \geq 0$ to the objective function of problem (11) to minimize the risk of difference between the presumed frequency deviation profile $\Delta\hat{\omega}(t+1)$ and the realized frequency deviation profile $\Delta\omega(t+1)$. The optimization problem for the system operator at each control time slot t can be formulated as follows.

$$\begin{aligned} & \text{minimize} && |\Delta\omega^{\text{reg}}(t) + \Delta\omega(t)| + \sum_{k=t+1}^T |\Delta\omega^{\text{reg}}(k) + \Delta\hat{\omega}(k)| \\ & \mathbf{p}_n^s(t), n \in \mathcal{N}, && \Delta\omega^{\text{reg}}(t), \Delta\omega^{\text{reg}}(k), k \in \mathcal{T}(t+1), \\ & \Delta\hat{\omega}(t+1), \eta && + \kappa \Gamma_\delta(\Delta\hat{\omega}(t+1), \eta) \end{aligned} \quad (17)$$

subject to constraints (1)–(10) for time slots $\{t, \dots, T\}$.

To transform problem (17) into a linear program, we introduce nonnegative auxiliary variables $\gamma(t)$ and $\gamma(k)$, $k \in \{t+1, \dots, T\}$ for the term $|\Delta\omega^{\text{reg}}(t) + \Delta\omega(t)|$ and $|\Delta\omega^{\text{reg}}(k) + \Delta\hat{\omega}(k)|$, respectively. We introduce nonnegative auxiliary variables $\lambda^j(k)$, $j \in \mathcal{J}$, $k \in \{t+1, \dots, T\}$ for the term $|\Delta\hat{\omega}(k) - \Delta\omega^j(k)|$ in $f(\Delta\hat{\omega}(t+1), \Delta\omega^j(t+1))$. We also introduce auxiliary variable $\mu^j(t)$, $j \in \mathcal{J}$ to upper bound each term $[f(\Delta\hat{\omega}(t+1), \Delta\omega^j(t+1)) - \eta]^+$. We define vectors $\boldsymbol{\gamma}(t) = (\gamma(t), \dots, \gamma(T))$, $\boldsymbol{\lambda}^j(t+1) = (\lambda^j(t+1), \dots, \lambda^j(T))$, $j \in \mathcal{J}$, and $\boldsymbol{\mu}(t+1) = (\mu^j(t+1), j \in \mathcal{J})$. Problem (17) can be rewritten as

$$\begin{aligned} & \text{minimize} && \sum_{\tau=t}^T \gamma(\tau) + \kappa \left(\eta + \sum_{j \in \mathcal{J}} \frac{\Pr\{\Delta\omega^j(t+1)\}}{(1-\delta)} \mu^j(t+1) \right) \\ & \mathbf{p}_n^s(t), n \in \mathcal{N}, && \Delta\hat{\omega}(t+1), \eta, \\ & \Delta\omega^{\text{reg}}(t), \Delta\omega^{\text{reg}}(k), k \in \mathcal{T}(t+1), && \boldsymbol{\gamma}(t), \boldsymbol{\lambda}^j(t+1), \boldsymbol{\mu}(t) \end{aligned} \quad (18)$$

subject to constraints (1)–(10) for time slots $\{t, \dots, T\}$,

$$\begin{aligned} & -\gamma(t) \leq \Delta\omega^{\text{reg}}(t) + \Delta\omega(t) \leq \gamma(t), \\ & -\gamma(k) \leq \Delta\omega^{\text{reg}}(k) + \Delta\hat{\omega}(k) \leq \gamma(k), \quad k \in \mathcal{T}(t+1), \\ & -\lambda^j(k) \leq \Delta\hat{\omega}(k) - \Delta\omega^j(k) \leq \lambda^j(k), \quad k \in \mathcal{T}(t+1), \\ & \sum_{k=t+1}^T \lambda^j(k) - \eta \leq \mu^j(t+1). \end{aligned}$$

Problem (18) is a linear program and can be solved efficiently to determine the optimal scheduling profile $\mathbf{p}_n^{s, \text{opt}}(t)$ of the energy storage system at bus n in each control time slot t .

IV. PERFORMANCE EVALUATION

We evaluate the performance of the proposed frequency regulation approach on an IEEE 37-bus distribution test feeder [15] with three energy storage systems. The test feeder is shown in Fig. 1. The equivalent virtual generator to model the transmission network is connected to the substation bus 37. For convenience, voltage magnitudes are in per-unit (pu) with a 4.8 kV base. The base power of the system is 100 kVA. The slack bus is the substation bus, i.e., its voltage magnitude is 1 pu and its phase angle is zero. The energy storage systems are located at buses 13, 23, and 31. We assume that no generator or frequency sensitive load is connected to buses within the distribution network, and thus we set the frequency bias factor to $\beta_n = 0, n = 1, \dots, 36$. The frequency bias factor β_n of the substation bus $n = 37$, where the virtual generator is connected, is set to 0.3483 pu/Hz [16, p. 24]. Since high frequency deviations occur during peak load hours, we consider a six-hour operation period and divide it into 24 frequency control time slots, where one control time slot is 15 minutes. To obtain the load profile over the operation cycle, we use the database for Ontario [17] over time interval [4 pm, 9 pm] on May 2, 2017. We scale the load demand to make the average demand at each bus over the operation cycle equal to its corresponding spot load specified in [15]. We use the measurement data in [18] to obtain $J = 50$ samples of frequency deviation. The confidence level δ is set to be 0.95. Unless stated otherwise, the weight coefficient κ is set to be 1.

We first present the frequency regulation performance when energy storage systems of different sizes are used. If the system operator has perfect knowledge about the frequency changes, then it determines the charging/discharging of the energy storage systems at the beginning of the operation cycle and schedules them to restore the frequency to its nominal value accordingly. If the system operator has uncertainty about the frequency changes, then it solves problem (18) at each time slot to regulate the frequency. Fig. 2(a) shows the results when the energy storage systems are small size with $E_{13}^{\max} = 10$ kWh, and $E_{23}^{\max} = E_{31}^{\max} = 5$ kWh. It can be observed that the system operator either with perfect knowledge or with uncertainty about the frequency changes cannot regulate the frequency in most of the time slots, due to the stringent operation constraints of the energy storage systems.

Fig. 2(b) shows the results when the energy storage systems are medium size with $E_{13}^{\max} = 50$ kWh, and $E_{23}^{\max} = E_{31}^{\max} = 30$ kWh. The system operator with perfect knowledge about the frequency changes can regulate the frequency in most of the time slots. In time slot 11, the frequency is not regulated because the energy storage systems discharge to be able to perform regulation during time slots 12 and 13 when charging is needed. With uncertainty about the frequency changes, the system operator can also regulate the frequency almost similar to the scenario with perfect knowledge except during time slots 10 to 13, when the frequency has experienced high deviations.

Fig. 2(c) shows the results when the energy storage systems are large size with $E_{13}^{\max} = 150$ kWh, and $E_{23}^{\max} = E_{31}^{\max} =$

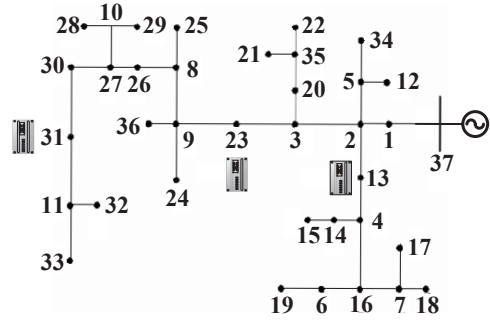


Fig. 1. IEEE 37-bus distribution test feeder used in the simulation, with the equivalent virtual generator connected to the substation bus 37, and three energy storage systems at buses 13, 23, and 31, respectively.

100 kWh. It can be observed that the frequency regulation performance is similar to the scenario with perfect knowledge except in a few time slots such as 8 and 18. Thus, we conclude that when the size of the energy storage systems decreases, the system operator may fail to restore the frequency during time slots with high frequency changes due to the operation limits of the energy storage systems and the uncertainty issues.

To further study the impact of the energy storage capacity on the frequency regulation performance, we compare the average regulated frequency deviation from the nominal value after performing the regulation with three energy storage systems of different sizes during the operation cycle, as shown in Fig. 3. The capacity and the initial charging energy level of the small, medium and large energy storage are set to be the same as the energy storage used in Fig. 2. We can observe that the regulated frequency deviation increases as the energy storage capacity decreases. As illustrated, when the size of the energy storage decreases by half, the regulated frequency deviations increases by 50%. When the size of the energy storage decreases by 90%, the regulated frequency deviations increases by 350%.

Finally, we study the impact of the weight coefficient κ on the frequency regulation performance. Fig. 4 shows the CVaR versus the regulated system frequency deviation from the nominal value, given the frequency deviations observed in Fig. 2. It can be observed that when κ increases from 0 to 10, the value of CVaR decreases from 1.39 Hz to 0.29 Hz. This indicates that the system operator becomes more conservative about the expected future frequency changes in the system when making current scheduling decisions for the energy storage systems to provide frequency regulation. As illustrated, being more conservative with a larger value of κ makes the system operator to reduce the expectations about the future frequency changes, and the deviation of the regulated system frequency from the nominal value thus increases.

V. CONCLUSION

In this paper, we formulated a linear program to schedule the energy storage systems in the distribution network to provide frequency regulation. We designed the ACE signals for secondary frequency regulation service, while taking into account the energy storage availability, the AC power flow in the distribution network as well as the uncertainties in

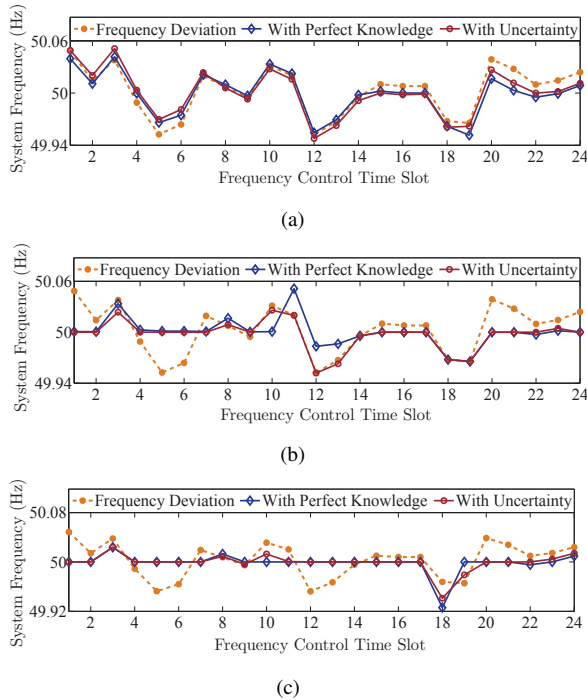


Fig. 2. Frequency regulation by using (a) three small energy storage systems with their initial energy level $E_{13}^{\text{init}} = 5$ kWh, $E_{23}^{\text{init}} = 2.5$ kWh, and $E_{31}^{\text{init}} = 5$ kWh, (b) three medium energy storage systems with their initial energy level $E_{13}^{\text{init}} = 25$ kWh, $E_{23}^{\text{init}} = 15$ kWh, and $E_{31}^{\text{init}} = 30$ kWh, (c) three large energy storage systems with their initial energy level $E_{13}^{\text{init}} = 100$ kWh, $E_{23}^{\text{init}} = 75$ kWh, and $E_{31}^{\text{init}} = 100$ kWh.

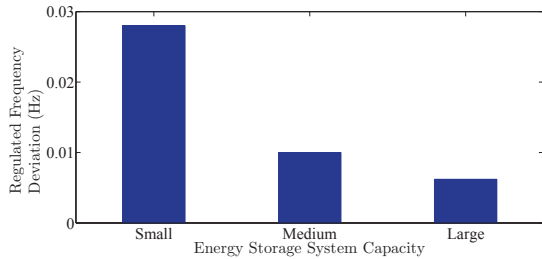


Fig. 3. The regulated frequency deviation after performing the regulation by using three energy storage systems with different sizes.

the frequency changes. Our problem formulation captured the risk of energy storage systems not being able to participate in the regulation service based on CVaR. By using linear approximation of the AC power flow model and sample average approximation of CVaR, our problem could be solved efficiently. Simulation results showed that our risk-averse model for the system operator can successfully schedule the energy storage systems to restore the current frequency deviation, while taking into account the risk of the energy storage system not being able to participate in the frequency regulation in the upcoming time slots.

ACKNOWLEDGEMENT

This work has been supported by the Natural Sciences and Engineering Research Council of Canada (NSERC).

REFERENCES

[1] B. J. Kirby, "Frequency regulation basics and trends," U.S. Department of Energy, Dec. 2005.

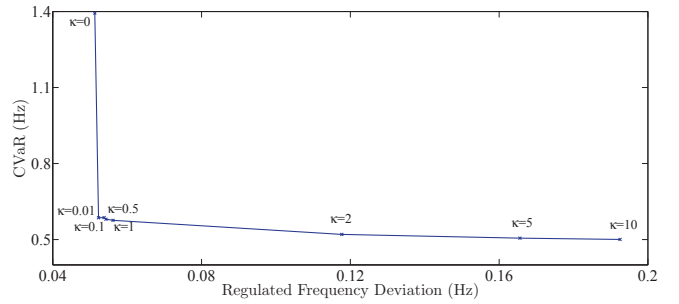


Fig. 4. The tradeoff between the regulated frequency deviations and CVaR when three small energy storage systems are used for frequency regulation with different weight coefficient κ .

[2] D. Hedberg, M. Emmett, G. Sodeberg, N. McIntire, R. Gramlich, and R. Kondziolka, "FERC order 890: What does it mean for the west?" National Association of Regulatory Utility Commissioners (NARUC), National Wind Coordinating Collaborative (NWCC), and the Western Governors Association, Tech. Rep., Feb. 2007.

[3] U.S. Federal Energy Regulatory Commission (FERC), "Frequency regulation compensation in organized wholesale power markets," Washington, DC, USA, FERC 755, Dockets RM11-7-000 AD10-11-000, Oct. 2011.

[4] M. Kintner-Meyer, "Regulatory policy and markets for energy storage in North America," *Proc. of the IEEE*, vol. 102, no. 7, pp. 1065–1072, Jul. 2014.

[5] S. Chen, T. Zhang, H. B. Gooi, R. D. Masiello, and W. Katzenstein, "Penetration rate and effectiveness studies of aggregated BESS for frequency regulation," *IEEE Trans. on Smart Grid*, vol. 7, no. 1, pp. 167–177, Jan. 2016.

[6] F. Zhang, Z. Hu, X. Xie, J. Zhang, and Y. Song, "Assessment of the effectiveness of energy storage resources in the frequency regulation of a single-area power system," accepted for publication in *IEEE Trans. on Power System*, 2017.

[7] Y. J. Zhang, C. Zhao, W. Tang, and S. H. Low, "Profit maximizing planning and control of battery energy storage systems for primary frequency control," accepted for publication in *IEEE Trans. on Smart Grid*, 2016.

[8] E. Yao, V. W. S. Wong, and R. Schober, "Robust frequency regulation capacity scheduling algorithm for electric vehicles," *IEEE Trans. on Smart Grid*, vol. 8, no. 2, pp. 984–997, Mar. 2017.

[9] G. He, Q. Chen, C. Kang, Q. Xia, and K. Poolla, "Cooperation of wind power and battery storage to provide frequency regulation in power markets," accepted for publication in *IEEE Trans. on Power Systems*, 2016.

[10] J. Tan and Y. Zhang, "Coordinated control strategy of a battery energy storage system to support a wind power plant providing multi-timescale frequency ancillary services," *IEEE Trans. on Sustainable Energy*, vol. 8, no. 3, pp. 1140–1153, Jul. 2017.

[11] D. Pudjianto, C. Ramsay, and G. Strbac, "Virtual power plant and system integration of distributed energy resources," *IET Renewable Power Generation*, vol. 1, no. 1, pp. 10–16, Mar. 2007.

[12] A. J. Wood, B. F. Wollenberg, and G. B. Sheblé, *Power Generation, Operation, and Control*, 3rd ed. John Wiley & Sons, 2013.

[13] N. Cai, Y. Tian, and J. Mitra, "Optimal branch numbering for UPFC benefit study," in *Proc. of North American Power Symposium (NAPS)*, Charlotte, NC, Oct. 2015.

[14] A. J. Conejo, M. Carrión, and J. M. Morales, *Decision Making Under Uncertainty in Electricity Markets*. Springer, 2010.

[15] "IEEE Power and Energy Society distribution test feeders," 2016. [Online]. Available: <http://ewh.ieee.org/soc/pes/dsacom/testfeeders/index.html>

[16] H. Bevrani, *Robust Power System Frequency Control*. Springer, 2009.

[17] IESO, "Hourly Ontario and market demands, year to date." [Online]. Available: www.ieso.com/power-data/data-directory

[18] FINGRID, "Frequency measurement data." [Online]. Available: [http://www.fingrid.fi/en/powersystem/Power system management/Maintainine of balance between electricity consumption and production/Frequency measurements data/Pages/default.aspx](http://www.fingrid.fi/en/powersystem/Power%20system%20management/Maintainine%20of%20balance%20between%20electricity%20consumption%20and%20production/Frequency%20measurements%20data/Pages/default.aspx)